Catalysis Science & Technology

PAPER

View Article Online
View Journal

Cite this: DOI: 10.1039/c4cy00551a

Elucidating the olefin formation mechanism in the methanol to olefin reaction over AlPO-18 and SAPO-18

Jingrun Chen,[ab] Jinzhe Li,[a] Cuiyu Yuan,[a] Shutao Xu,[a] Yingxu Wei,*[a] Quanyi Wang,[ab] You Zhou,[ab] Jinbang Wang,[ab] Mozhi Zhang,[ab] Yanli He,[a] Shuliang Xu[a] and Zhongmin Liu*[a]

Received 29th April 2014,
Accepted 10th June 2014

DOI: 10.1039/c4cy00551a

www.rsc.org/catalysis

The mechanism of the methanol to olefin (MTO) reaction over AlPO-18 (without Brønsted acid sites) and two SAPO-18 (with different Brønsted acid site densities) catalysts has been investigated. The Brønsted acid site density of AlPO-18 and SAPO-18 catalysts was determined by ^{1}H MAS NMR spectroscopy. Methanol conversion over the catalysts showed that the catalytic activity of the catalysts was strongly influenced by their Brønsted acid site density. Using ^{13}C magic angle spinning (MAS) NMR, we directly observed the pentamethylcyclopentenyl cation (pentaMCP^{+}) over SAPO-18 under real MTO reaction conditions, but no carbenium ion was detected over AlPO-18. Furthermore, analysis of confined organics by ^{13}C MAS NMR and GC-MS clearly demonstrated that higher Brønsted acid site density improved the formation and accumulation of some important and reactive hydrocarbon pool species, such as pentaMCP^{+} and polymethylbenzenes. With the aid of the ^{12}C/^{13}C-methanol switch technique, the detailed olefin formation mechanism was elucidated. During the MTO reaction, light olefin generation over SAPO-18 mainly followed the aromatic-based hydrocarbon pool mechanism; however, the olefin methylation and cracking mechanism accounted for the production of light olefins over AlPO-18.

1. Introduction

As an alternative route for the production of light olefins from non-oil resources, the methanol to olefin (MTO) reaction has received much attention from both academia and industry.[1–11] The MTO process has been proven to be completely successful in China using the DMTO technology developed by the Dalian Institute of Chemical Physics.[7,12] Although the excellent performance of methanol conversion to light olefins over acidic zeolites or silicoaluminophosphate (SAPO) molecular sieves (*e.g.* SAPO-34 used in the DMTO process) has been undoubtedly confirmed, due to the extremely complicated reaction route and network of MTO reaction, elucidating the reaction mechanism remains a great challenge.

Based on the intensive mechanistic studies of the MTO reaction,[1–11,13–15] C–C bond formation by direct coupling of C1 species derived from methanol has been proven to be unfavourable owing to the extraordinarily high energy barrier and unstable reaction intermediates.[13–15] An indirect mechanism, the hydrocarbon pool (HP) mechanism,[16–18] has been confirmed based on experimental observations[19–27] as well as theoretical calculations[28–32] and gained general acceptance. According to the HP mechanism, methanol is continuously added to the HP species confined in the catalyst and light olefins are split off from these species. Polymethylbenzenes and the corresponding carbenium ions have been proposed to be the main reactive HP species.[19–22,33–36] Using isotopic switch experiments, pentamethylbenzene and hexamethylbenzene have been found to be more reactive than the lower methylbenzenes (toluene, xylene and trimethylbenzene) over SAPO-34 and H-beta catalysts, while the lower methylbenzenes were shown to be more active than the higher methylbenzenes over H-ZSM-5.[20,23–25,37] However, detailed mechanistic investigations revealed that C_{3+} alkenes were formed through alkene methylation and cracking reaction over H-ZSM-5 besides ethene generation following the aromatic-based HP mechanism.[23–25,37] Further investigations proved that methanol conversion over H-ZSM-22 mainly followed the alkene methylation and cracking reaction mechanism.[27,38] Recently, Wang *et al.* found that the olefin methylation and cracking mechanism was dominantly responsible for the generation of olefin products over SAPO-41 with one-dimensional 10-membered ring pores.[39]

In the proposed aromatic-based HP mechanism, Brønsted acidity is closely related to the formation of important

[a] National Engineering Laboratory for Methanol to olefins, Dalian National Laboratory for Clean Energy, Dalian Institute of Chemical Physics, Chinese Academy of Sciences, Dalian 116023, PR China. E-mail: liuzm@dicp.ac.cn, weiyx@dicp.ac.cn; Fax: +86 411 84691570; Tel: +86 411 84379335
[b] University of Chinese Academy of Sciences, Beijing 100049, PR China

intermediates (polymethylbenzenes and the corresponding carbenium ions) and light olefin generation during the MTO conversion.[7,8,34–36,40–44] For example, Dai *et al.* found that the density of Brønsted acid sites strongly affected the activity and lifetime of the MTO catalysts, and higher Brønsted acid site density favoured the formation of HP species, over which an enhanced methanol conversion could be achieved.[40] Dai *et al.* also found that incorporation of a small amount of silica into AlPO-34 had a positive effect on the activity and product selectivity of the MTO conversion and also contributed to the prolongation of the catalyst lifetime, which they attributed to the formation of HP species with a higher content of dienes and a small amount of large aromatics.[42]

For the acid-catalyzed MTO reaction with a complicated reaction mechanism, it is necessary to understand how the Brønsted acid site density of the catalyst affects the reaction route of methanol conversion to light olefins. Especially, when the catalyst acidity is very weak, as in AlPO molecular sieves, due to the difficulty of HP species formation, the MTO reaction following the HP mechanism is very difficult to be realized over this catalyst.

AlPO-18 is an aluminophosphate molecular sieve with AEI cages and 8-membered ring pore openings. If silicon impurities are introduced during the synthesis procedure of AlPO-18, Brønsted acid sites can be created.[45] These acid sites are a result of the substitution of P by Si atoms in the AlPO-18 framework. The substitution leads to the formation of negative framework charges, which are then charge-balanced by the protons from the bridge hydroxyl groups, the Brønsted acid sites of SAPO molecular sieves.[45] SAPO-18, possessing the same framework as that of AlPO-18, displays a similar catalytic performance to that of SAPO-34 in the MTO reaction.[45–48] SAPO-18 with varied framework silicon incorporation is comparatively easy to be synthesized, and hence the varied Brønsted acid site density.[45,46]

Thus in this contribution, AlPO-18 and SAPO-18 molecular sieves with different Brønsted acid densities were employed as the catalysts in the MTO reaction. The Brønsted acid site density of the AlPO-18 and SAPO-18 catalysts used in this study was determined by ^{1}H MAS NMR spectroscopy. The study of the MTO reaction over AlPO-18 and SAPO-18 with identical topology structures but different Brønsted acid densities would give typical results for elucidating the effect of the Brønsted acid site density of the catalysts on the olefin formation mechanism of the MTO reaction.

2. Experimental

2.1 Synthesis of AlPO-18 and SAPO-18 samples

The AlPO-18 and SAPO-18 samples employed in this study were synthesized hydrothermally following the procedure described in the literature.[45,46] Aluminium isopropoxide, phosphoric acid and colloidal silica were used as the sources of aluminium, phosphorus and silicon, respectively. The chemical compositions of the starting gel are shown in Table 1. The obtained samples were named AlPO-18, SAPO-18-1 and SAPO-18-2 depending on their Si contents.

2.2 Characterization

The powder XRD patterns were recorded using a PANalytical X'Pert PRO X-ray diffractometer with Cu Kα radiation (λ = 1.54059 Å) operating at 40 kV and 40 mA.

The chemical composition of the solid samples was determined with a Philips Magix-601 X-ray fluorescence (XRF) spectrometer.

The crystal morphology was observed by scanning electron microscopy (SEM, Hitachi S-3400N).

^{13}C solid-state MAS NMR experiments were performed using a Bruker Avance III 600 spectrometer equipped with a 14.1 T wide-bore magnet and a 4 mm MAS probe. The resonance frequencies were 150.9 MHz for ^{13}C. ^{13}C MAS NMR spectra were recorded using high-power proton decoupling with a spinning rate of 12 kHz. 2700 scans were accumulated with a $\pi/4$ pulse width of 1.8 μs and a 4 s recycle delay. The chemical shifts were referenced to adamantane with the upfield methine peak at 29.5 ppm.

^{1}H MAS NMR spectroscopy was performed using a Varian Infinity plus-400 spectrometer equipped with a 9.4 T wide-bore magnet. ^{1}H MAS NMR spectra were recorded using a spin-echo program and a 4 mm MAS probe. The pulse width was 2.2 μs for a $\pi/4$ pulse, and 32 scans were accumulated with a 10 s recycle delay. Before the ^{1}H MAS NMR measurements, samples were dehydrated at 400 °C and at a pressure below 10^{-3} Pa for 20 h. Samples were spun at 12 kHz, and chemical shifts were referenced to adamantane at 1.74 ppm. The software Dmfit was employed for deconvolution using fitted Gaussian–Lorentzian line shapes. ^{1}H/^{27}Al TRAPDOR (transfer of populations in double resonance) experiments were performed with a spin-echo pulse applied to the ^{1}H channel and aluminium was irradiated simultaneously during the first τ period. The excitation pulse length was

Table 1 Molar composition of the initial gel and synthesized products of AlPO-18 and SAPO-18

	Starting gel composition	Product composition		
Sample	Molar composition	Molar composition[a]	Si/(Si + P + Al)	Concentration of B acid[b] (mmol g^{-1})
AlPO-18	$1.0P_2O_3 : 1.0Al_2O_3$	$Al_{0.508}P_{0.492}O_2$	0	0
SAPO-18-1	$1.0P_2O_3 : 0.8Al_2O_3 : 0.05SiO_2$	$Al_{0.496}P_{0.489}Si_{0.014}O_2$	0.014	0.246
SAPO-18-2	$1.0P_2O_3 : 0.9Al_2O_3 : 0.2SiO_2$	$Al_{0.484}P_{0.464}Si_{0.052}O_2$	0.052	0.568

[a] Determined by X-ray fluorescence (XRF) spectrometry. [b] Determined by ^{1}H MAS NMR spectroscopy.

2.6 μs (π/2), and τ was set to one rotor period. The ^{27}Al irradiation field was about 60 kHz.

The temperature-programmed ammonia desorption (NH_3-TPD) experiments were conducted using a Micromeritics Autochem II 2920 device. 100 mg of the sample particles (40–60 mesh) were loaded into a U-quartz tube and pretreated at 650 °C for 60 min under helium flow. After cooling to 100 °C, NH_3 was introduced to saturate the sample surface and then the sample was purged with He for 30 min to remove the weakly adsorbed NH_3 molecules. The measurement of NH_3 desorption was performed from 100 °C to 700 °C (10 °C min^{-1}) under He flow (20 ml min^{-1}).

2.3 MTO reaction

Methanol conversion was performed in a fixed-bed quartz tubular reactor at atmospheric pressure. A catalyst sample of 100 mg (60–80 mesh) was loaded into the reactor and the reactions were carried out at 300 °C and 400 °C. Methanol was fed by passing helium through a saturation evaporator with a WHSV of 2.0 h^{-1}. The reaction products were analyzed by an on-line gas chromatograph (Agilent GC 7890A) equipped with an HP-PLOT Q capillary column and a FID detector. The conversion and selectivity were calculated on a CH_2 basis. Dimethyl ether (DME) was considered as a reactant in the calculation.

2.4 Confined organics analysis

Organic species trapped in the cages of the AlPO-18 and SAPO-18 molecular sieves during the reaction were analyzed following the procedures described in the literature.[49,50] The spent catalysts were dissolved in 20% hydrofluoric acid solution. The organic phase was extracted with dichloromethane (CH_2Cl_2) and then analyzed using an Agilent 7890A/5975C GC/MSD equipped with an HP-5 capillary column.

The confined organics in the catalyst sample during methanol conversion were also measured by ^{13}C solid-state MAS NMR employing ^{13}C-methanol as the reactant. ^{13}C-methanol was fed into the reactor for a predetermined time and then the reactor was removed from the feeding line; the catalyst was then cooled quickly by putting the catalyst particles into a vessel containing liquid nitrogen. Finally, the cooled catalyst was transferred to an NMR rotor in the glove box without exposure to ambient air.

2.5 ^{12}C/^{13}C-methanol switch experiments

In the ^{12}C/^{13}C-methanol switch experiments, after the ^{12}C-methanol was fed by passing the carrier gas (He) through a methanol saturation evaporator maintained at 14 °C into the reactor at the reaction temperature for 25 min to build up ^{12}C-HP species in the cages of AlPO-18 and SAPO-18, the feeding of ^{12}C-methanol was stopped and the reactant was switched to ^{13}C-methanol (fed by passing the carrier gas (He) through a ^{13}C-methanol saturation evaporator) for 1 min; then, the reaction was stopped and the catalyst was cooled quickly by putting the catalyst particles into a vessel containing liquid nitrogen. The WHSV of methanol was 2.0 h^{-1}. The isotopic distribution of effluents and the materials confined in the catalyst were analyzed using an Agilent 7890A/5975C GC/MSD.

3. Results and discussion

3.1 Characterization of AlPO-18 and SAPO-18 catalysts

Fig. 1 shows the XRD patterns of the as-synthesized AlPO-18 and SAPO-18 samples, which are in good agreement with those of the reports and correspond to the AEI structure.[2,45,46] The SEM images of AlPO-18 and SAPO-18 samples are shown in Fig. 2; the AlPO-18 and SAPO-18 particles all appear as hexagonal prisms *ca.* 800 nm in length and *ca.* 200 nm in width packed by flaky crystals. The chemical compositions of the calcined AlPO-18 and SAPO-18 catalysts are given in Table 1.

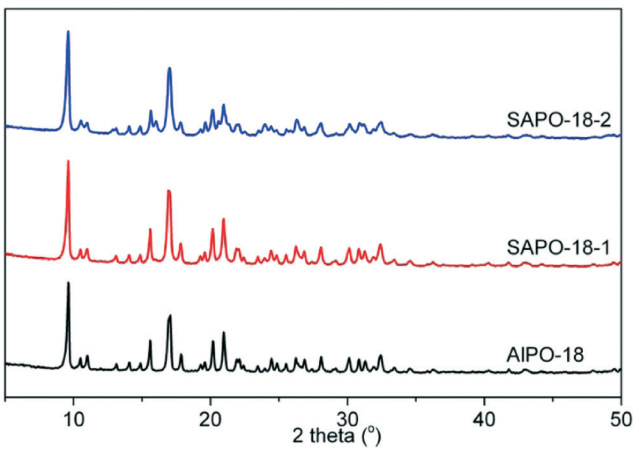

Fig. 1 XRD patterns of the synthesized AlPO-18 and SAPO-18 samples.

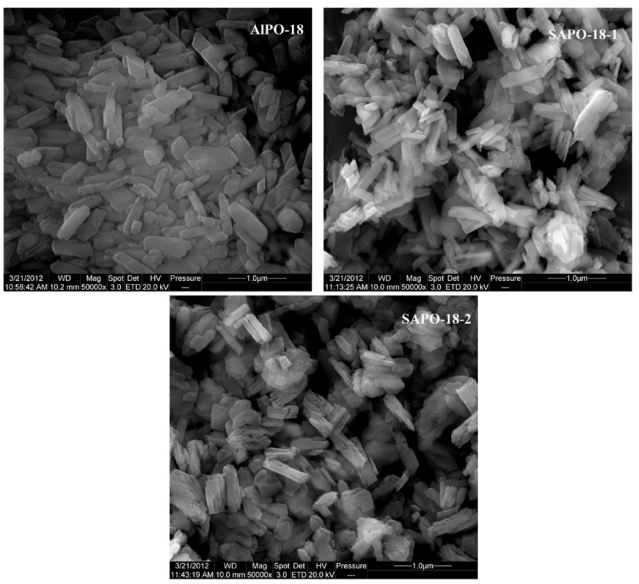

Fig. 2 SEM images of the as-synthesized AlPO-18 and SAPO-18 samples.

The Brønsted acid sites of the calcined AlPO-18 and SAPO-18 catalysts were characterized by means of ^{1}H MAS NMR spectroscopy. The obtained spectra are shown in Fig. 3(a). Three signals appear in the spectra of the two SAPO-18 samples. The signals at 1.6 and 0.1 ppm with low intensity are assigned to Si(OH) and Al(OH), respectively, and the signal at 3.7 ppm is ascribed to bridge hydroxyl groups (Si(OH)Al), indicating the presence of Brønsted acid sites in the synthesized SAPO-18-1 and SAPO-18-2. The signals from Si(OH) (1.6 ppm) and Al(OH) (0.1 ppm) are also present in the spectrum of AlPO-18, but the signal from bridge hydroxyl groups is absent, indicating the non-acidity of AlPO-18 with neutral framework. Instead, a signal at 3.3 ppm appears in the spectrum of AlPO-18. The TRAPDOR (transfer of populations in double resonance) technique was employed to determine its assignment. Under strong aluminium irradiation during the spin-echo pulse sequence applied to the proton, the signal of the proton groups that are strongly coupled to aluminium will be significantly suppressed while those of the other protons will be unchanged. Therefore, the technique offers the possibility to differentiate between the OH signals of species close to an aluminium atom and those of species that are further away. After ^{27}Al irradiation, the signals at 3.3 ppm and 1.3 ppm (the background of probe) maintained their intensity (Fig. 3(b)) but the signal at 0.1 ppm weakened, indicating that the signal at 3.3 ppm is from P(OH) and not from Si(OH)Al. P(OH) cannot be observed in the spectra of SAPO-18 due to its signal being overlapped by the signal of Si(OH)Al.

After quantifying the concentration of hydroxyl groups using the signal intensity, the Brønsted acid site density was determined to be 0.246 mmol g^{-1} and 0.568 mmol g^{-1} for SAPO-18-1 and SAPO-18-2, respectively, consistent with their silicon content.

NH_3-TPD curves of AlPO-18 and SAPO-18 samples are shown in Fig. 4. For AlPO-18, only one desorption peak at *ca.* 165 °C is observed, assigned to the desorption of physisorbed NH_3 and NH_3 adsorbed on lattice defects or terminal Si(OH) and Al(OH). For SAPO-18-1 and SAPO-18-2 catalysts, there are two desorption peaks. Aside from the low-temperature desorption peak at the same temperature range (*ca.* 160–170 °C) as that of AlPO-18, a high-temperature desorption peak at *ca.* 330–360 °C is observed, corresponding to the NH_3 desorption from the Brønsted acid sites, the bridge hydroxyl groups Si(OH)Al, of SAPO-18-1 and SAPO-18-2 catalysts, confirmed by ^{1}H MAS NMR, which behave as important active sites in acid-catalyzed reactions. As can be seen in Fig. 4, SAPO-18-2 with higher silicon content presents higher Brønsted acid site density than SAPO-18-1. One can also notice a significant difference in the integral amount of the low-temperature desorbed NH_3 from AlPO-18, SAPO-18-1 and SAPO-18-2. Si incorporation into the AlPO framework generates bridge hydroxyl groups. At the same time, Si incorporation may also cause more lattice defects in the crystals and more terminal hydroxyls, such as Si(OH), Al(OH) or P(OH). The varying desorption of NH_3 from these defects or terminal hydroxyls as shown in the NH_3-TPD profiles illustrates the difference

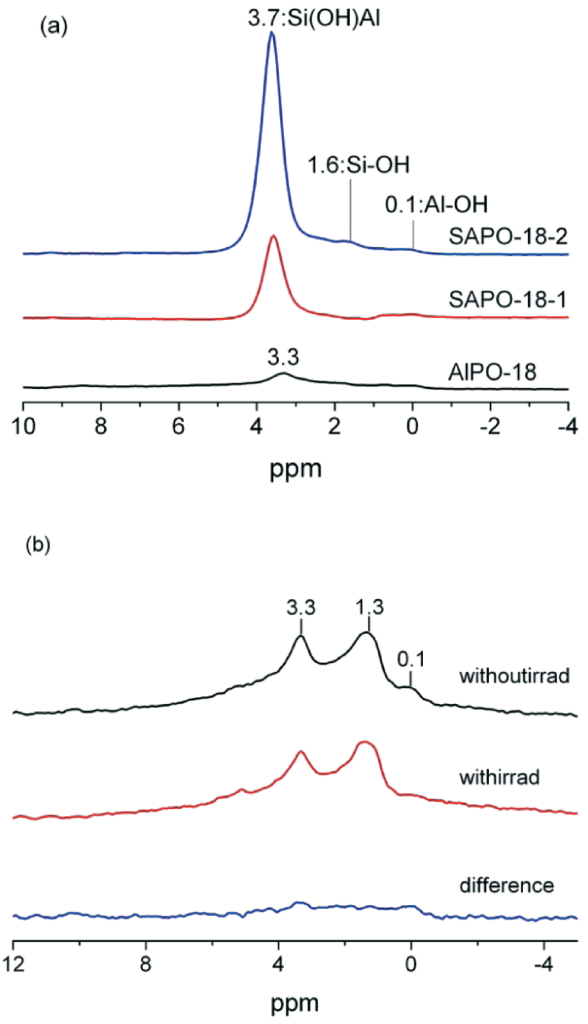

Fig. 3 (a) ^{1}H MAS NMR spectra of the calcined AlPO-18 and SAPO-18 catalysts (background subtraction has been performed). (b) ^{1}H/^{27}Al TRAPDOR spectra of AlPO-18.

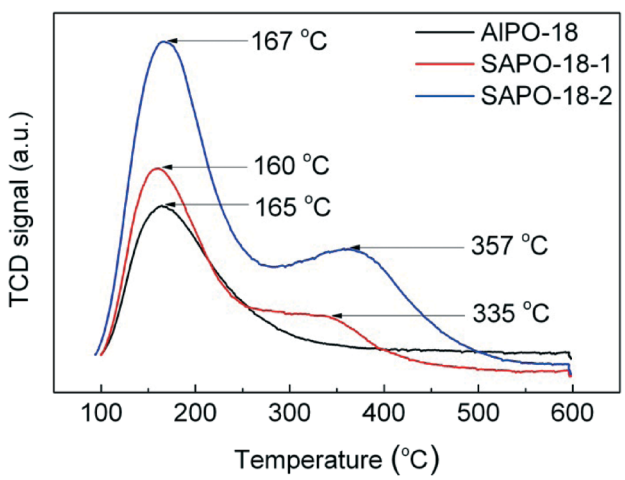

Fig. 4 NH_3-TPD profiles of the synthesized AlPO-18 and SAPO-18 catalysts.

between the three catalysts with different Si contents besides their Brønsted acidity.

3.2 Catalytic performance of MTO reaction over AlPO-18 and SAPO-18 catalysts

Fig. 5 shows the conversion of methanol with time-on-stream over AlPO-18 and SAPO-18. An extremely low conversion of methanol (less than 0.1%) is obtained over AlPO-18 at 300 °C. Even at an increased reaction temperature, the conversion over AlPO-18 is still very low, that is, about 3% methanol is transformed over AlPO-18 at 400 °C. In comparison, methanol conversion over SAPO-18-1 and SAPO-18-2 is much higher. For the reaction performed over SAPO-18 catalysts with different Brønsted acid site densities at 300 °C, an obvious induction period is observed. This is very similar to our previous studies of MTO conversion over the SAPO-34 and SAPO-35 catalysts at 300 °C.[51,52] During the induction period, the HP species, the active reaction centres of methanol conversion, are formed, and with the accumulation of these HP species in the cages, the reaction activity is improved.[2] The long induction period reflects the very slow rates of the formation and intensification of the active intermediates at low reaction temperature. Notably, maximum methanol conversion (nearly 17%) is achieved over SAPO-18-1 after a time-on-stream of 26 min at 300 °C, but for SAPO-18-2 with higher Brønsted acid density, a maximum methanol conversion of 50% is obtained at 300 °C after a time-on-stream of 26 min. This clearly demonstrates that higher Brønsted acid site density can improve the methanol conversion.

Product distributions of the MTO reaction over the AlPO-18 and SAPO-18 catalysts are shown in Fig. 6. For the three catalysts, light olefins including ethene, propene and butene are the main products, indicating that even with different Brønsted acid site densities, the AlPO-18 and SAPO-18 catalysts employed in the study are very selective catalysts for

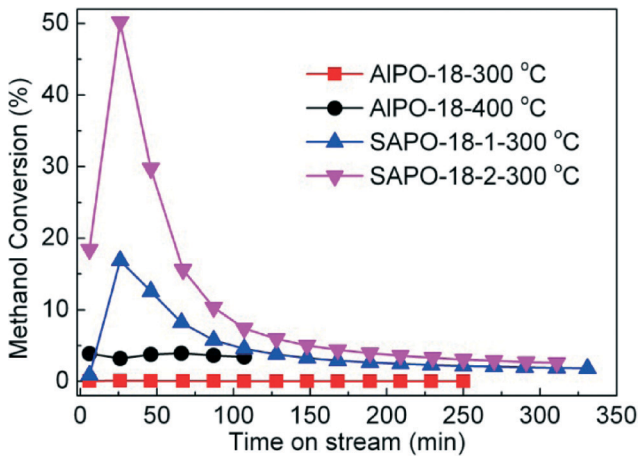

Fig. 5 Methanol conversion variation with time-on-stream over the AlPO-18 and SAPO-18 catalysts with different Brønsted acid site densities at 300 °C and 400 °C. Experimental conditions: WHSV = 2 h^{-1}; catalyst weight = 100 mg.

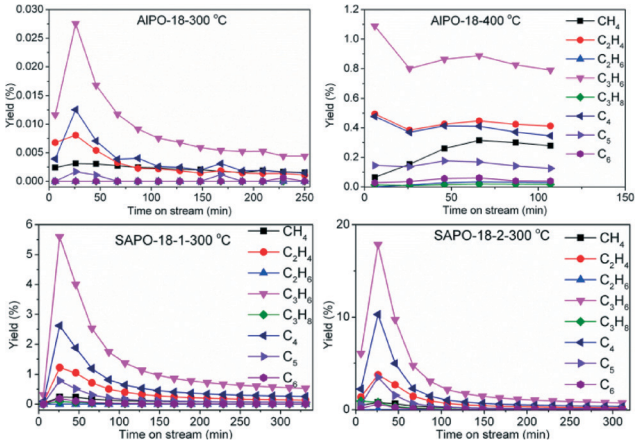

Fig. 6 Product distribution of the MTO reaction over the AlPO-18 and SAPO-18 catalysts with different Brønsted acid site densities at 300 °C and 400 °C. Experimental conditions: WHSV = 2 h^{-1}; catalyst weight = 100 mg.

the production of light olefins from methanol. Propene is always predominantly formed among the hydrocarbon products, and ethene selectivity is always comparable with butene selectivity and lower than propene selectivity. It is also noteworthy that very slight methanol transformation occurs over the AlPO-18 catalyst without Brønsted acid sites and that the main products are light olefins. The reactivity of AlPO-18 is possibly related to the surface defects or terminal hydroxyl groups. Besides the formation of C_2–C_4 light olefins, methane selectivity is relatively high over AlPO-18, which implies that some H-deficient species such as aromatic compounds are generated from the H-transfer reaction simultaneously and retained in the cages of AlPO-18.

3.3 ^{13}C MAS NMR spectra of retained organic species in AlPO-18 and SAPO-18 catalysts

Fig. 7 shows the ^{13}C MAS NMR spectra of the retained organic species in AlPO-18 and SAPO-18 catalysts after continuous-flow ^{13}C-methanol reaction (AlPO-18 at 400 °C for 25 min; SAPO-18-1 and SAPO-18-2 at 300 °C for 20 min). Considering the extremely low methanol conversion (less than 0.1%) over AlPO-18 at 300 °C, we conducted a ^{13}C MAS NMR study of ^{13}C-methanol conversion over AlPO-18 at 400 °C (methanol conversion higher than 3%) to make sure that the results are comparable. Diamondoid hydrocarbons, such as methyl-adamantanes (10–50 ppm), and alkylated aromatics, such as methylbenzenes (120–140 ppm),[4,51] are the most predominantly formed species among the organics retained in SAPO-18-2; the adsorbed methanol at 52 ppm can also be observed over this catalyst. Among the organics retained in the SAPO-18-1 catalyst, the adsorbed methanol at 52 ppm and dimethyl ether (DME) at 60.5 ppm appear as the main organics, and the signals of diamondoid hydrocarbons as well as those of alkylated aromatics can also be detected in very low intensity in the spectrum of the SAPO-18-1 catalyst. But for AlPO-18, the very strong signal at 52 ppm from the

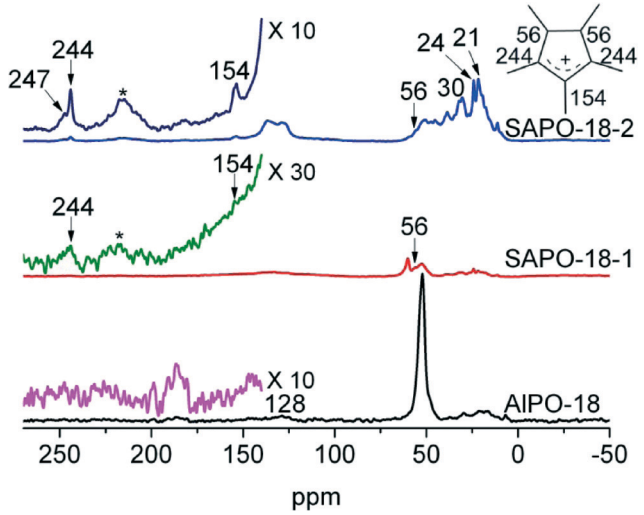

Fig. 7 ^{13}C MAS NMR spectra of the retained organic species in the AlPO-18 and SAPO-18 catalysts with different Brønsted acid site densities after continuous-flow ^{13}C-methanol reaction (AlPO-18 at 400 °C for 25 min; SAPO-18-1 and SAPO-18-2 at 300 °C for 20 min). The asterisk denotes spinning sidebands.

adsorbed methanol corresponds to the very low methanol conversion over AlPO-18 under these reaction conditions; in addition, some weak signals appear in the spectral region between 10–50 ppm. A previous report concerning a ^{13}C MAS NMR study of methanol conversion over SAPO-34 showed that the ^{13}C signals at 23, 127 and 136 ppm indicated the presence of alkylated aromatics,[51] such as methylbenzenes, so the signals between 10 and 50 ppm in the ^{13}C MAS NMR spectra of AlPO-18 can be assigned to carbon atoms from alkyl groups of the retained aromatics. The very low intensity signal at 128 ppm can be assigned to carbon atoms in the benzene ring. For the two SAPO-18 catalysts, besides the stable organic species mentioned above, some weak signals appear in the downfield region (140–250 ppm) with the characteristic chemical shift at about 240–250 and 154 ppm. The appearance of the resonance peaks at 240–250, 154, and 56 ppm in the ^{13}C MAS NMR spectra of the two SAPO-18 catalysts implies the formation of the polymethylcyclopentenyl cation over the two SAPO-18 catalysts;[53,54] on the other hand, these signals representing carbenium ions are not found in the ^{13}C MAS NMR spectra of AlPO-18 after ^{13}C-methanol reaction.

In our previous report, the solid-state NMR technique was employed to observe the carbenium formation over DNL-6, H-SAPO-34 and H-SSZ-13 catalysts under real MTO reaction conditions. According to our previous work, the polymethylcyclopentenyl cation observed in the present study can be ascribed to the pentamethylcyclopentenyl cation (pentaMCP$^+$).[34,35] The carbenium ion, pentaMCP$^+$, as the protonated form of pentamethylcyclopentadiene, is believed to be a very important reaction intermediate during MTO conversion.[35] In the present study, direct observation of pentaMCP$^+$ was also realized during the methanol conversion over SAPO-18-1 and SAPO-18-2 catalysts under real MTO reaction conditions but no carbenium ions were observed over AlPO-18 without Brønsted acid sites. Furthermore, the concentration of pentaMCP$^+$ varies with the Brønsted acid site density of the catalysts, 0.166 mmol g^{-1} over SAPO-18-1 and 0.378 mmol g^{-1} over the SAPO-18-2 catalyst, clearly demonstrating that higher Brønsted acid site density will accelerate the formation and accumulation of pentaMCP$^+$. At the same time, another kind of important carbenium ion, benzenium ions, which have been confirmed by ^{13}C solid-state NMR in our previous study,[34,35] was not detected in the present work, possibly due to their high reactivity and extreme instability during the reaction; while one should still note the signal of neutral methylbenzenes with chemical shifts of 120–140 ppm, the signal of the deprotonated form of the benzenium ion is intensified with the increasing Brønsted acid site density of SAPO-18. This observation indicates that the high Brønsted acid site density of SAPO-18-2 resulting from the larger amount of Si incorporated improves the formation of important reactive HP species during the MTO reaction such as the pentaMCP$^+$ and polymethylbenzenes which behave as important intermediates for light olefin elimination. For AlPO-18, owing to the absence of Brønsted acid sites, carbenium ions cannot form and the reaction route following the HP mechanism is not feasible over this catalyst. For this reason, AlPO-18 presents the lowest reactivity among the three catalysts.

3.4 ^{12}C/^{13}C-methanol switch experiments

^{12}C/^{13}C-methanol isotopic switch experiments provide insight into the reactivity of confined organic materials in the catalysts. By using this technique, reactive HP species can be distinguished from the inactive species in the working catalyst. Among the confined organics in the catalyst upon which ^{13}C-methanol is fed, the organic reaction centres would be more active towards ^{13}C-methanol than the other species and thus will contain more ^{13}C atoms from the ^{13}C-methanol feed after the switch experiment.[7]

The organic materials confined in the catalysts were analyzed by GC-MS and the results are given in Fig. 8. The reaction is performed over the two SAPO-18 catalysts at 300 °C, while the reaction temperature over AlPO-18 is 400 °C to achieve an appropriate methanol conversion. Methyl-substituted benzenes from toluene to hexamethylbenzene and methyl-substituted adamantanes can be found in the two SAPO-18 catalysts. Only trace amounts of pentamethylbenzene (pentaMB) and hexamethylbenzene (hexaMB) can be detected in the AlPO-18 catalyst, which is supposed to result from some possible secondary reaction of olefin products, such as oligomerization, cyclization and hydrogen transfer.[1] The peak intensity based on the addition of an internal standard is employed to compare the formation of confined organics. The results show that higher Brønsted acid site density favours the formation and accumulation of the reactive polymethylbenzenes. This is consistent with the variation of polymethylbenzene formation with the Brønsted acid site density of the catalysts measured by the ^{13}C MAS NMR spectra.

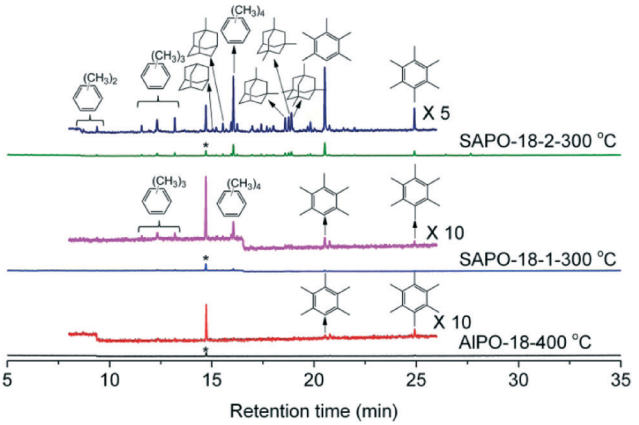

Fig. 8 GC-MS chromatograms of the organic species retained in the AlPO-18 and SAPO-18 catalysts with different Brønsted acid site densities after 25 min of ^{12}C-methanol reaction followed by 1 min of ^{13}C-methanol reaction (AlPO-18 at 400 °C; SAPO-18-1 and SAPO-18-2 at 300 °C). Experimental conditions: WHSV = 2 h^{-1}; catalyst weight = 100 mg.

Fig. 9 displays the total ^{13}C contents of the effluent olefin products and confined organic materials in the catalyst after the ^{12}C/^{13}C-methanol switch experiments which were conducted with ^{12}C-methanol feed for 25 min followed by ^{13}C-methanol reaction for 1 min. The detailed isotopomer distribution of the olefins and confined polymethylbenzenes formed in the ^{12}C/^{13}C-methanol switch experiments is illustrated in Fig. 10.

As for SAPO-18, most of the isotopomers of generated olefins and confined methylbenzenes over SAPO-18 contain ^{13}C and ^{12}C atoms (Fig. 10). The ^{13}C content of the gas-phase olefins is close to that of the confined polymethylbenzenes (such as hexaMB and pentaMB). Especially, hexaMB exhibits the highest ^{13}C content among the polymethylbenzenes in SAPO-18-2 with the highest Brønsted acid site density, and its high reactivity as an HP species is consistent with the report over SAPO-34.[19–21] It was also found that the isotopomers of hexaMB confined in AlPO-18, SAPO-18-1 and SAPO-18-2 exhibit no random distribution. For hexaMB retained in SAPO-18-2 with the highest Brønsted acid site density, the fraction of hexaMB isotopomers increases with the number of ^{13}C atoms included in the hexaMB isotopomers, and the isotopomer containing 12 ^{13}C atoms shows the highest content. Therefore, hexaMB is highly reactive towards the feeding of ^{13}C-methanol over SAPO-18-2. The calculated fraction of hexaMB isotopomers confined in SAPO-18-1 exhibits no obvious regulation, possibly caused by the low intensity of hexaMB confined in SAPO-18-1; however, one can still observe the relatively high content of the isotopomer containing 11 or 12 ^{13}C atoms. These results suggest that the aromatic-based HP mechanism is responsible for the conversion of methanol to light olefins over SAPO-18. In combination with the observation of pentaMCP$^+$ over SAPO-18 catalysts by ^{13}C MAS NMR (Fig. 7), methanol conversion under these conditions may follow the pairing route according to the HP mechanism, with involvement of 5-membered and 6-membered ring intermediates.

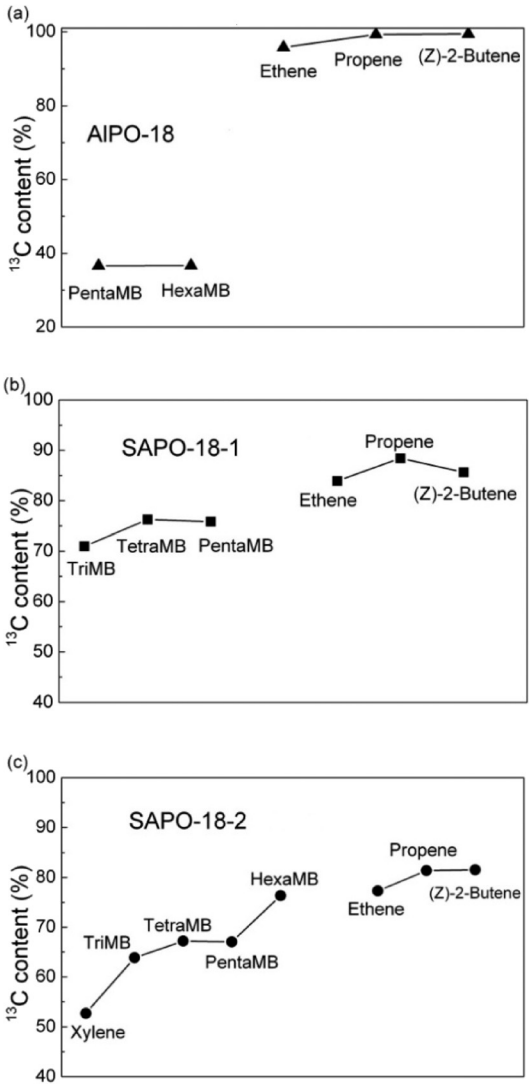

Fig. 9 ^{13}C content of the effluent light olefins and retained polymethylbenzenes confined in the AlPO-18 (a), SAPO-18-1 (b) and SAPO-18-2 (c) catalysts after 25 min of ^{12}C-methanol reaction followed by 1 min of ^{13}C-methanol reaction over AlPO-18 at 400 °C and SAPO-18-1 and SAPO-18-2 at 300 °C. Experimental conditions: WHSV = 2 h^{-1}; catalyst weight = 100 mg.

It should be noted that over the SAPO-18-1 catalyst with a relatively low Brønsted acid site density, the ^{13}C content of olefins among the gas-phase products is slightly higher than that of confined polymethylbenzenes. This difference becomes more dominant for the results over AlPO-18. The ^{13}C content of the olefin products is higher than 90%, while the ^{13}C contents of pentaMB and hexaMB are less than 40%. These results are consistent with the observation over H-ZSM-22.[27,38] The previous studies showed that aromatic compounds in the channel of the H-ZSM-22 catalyst are almost inactive for methanol conversion to light olefins, and the light olefins are much more reactive towards the feeding of ^{13}C-methanol than the retained polymethylbenzenes; therefore methanol conversion over the H-ZSM-22 catalyst

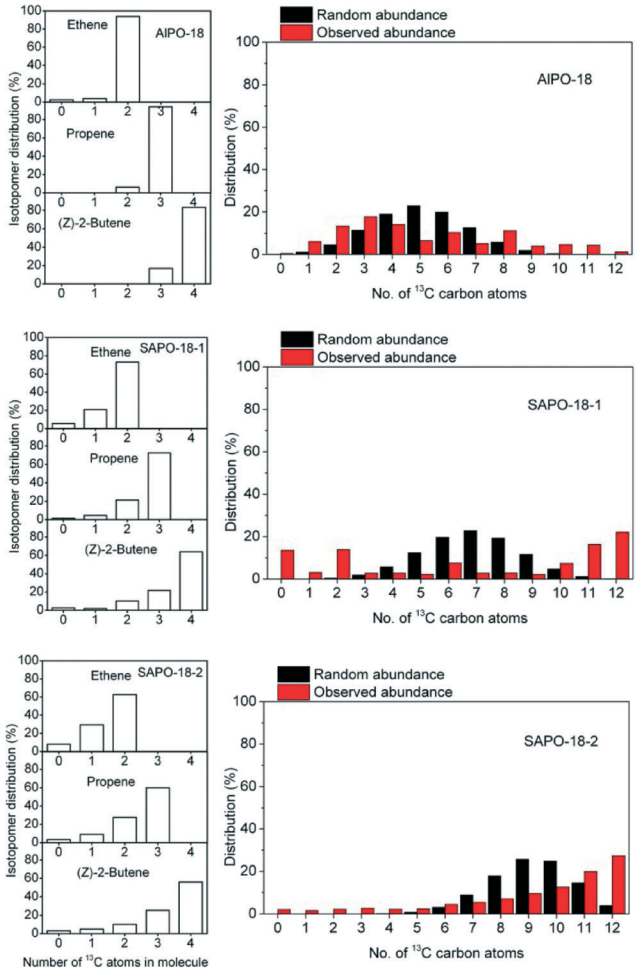

Fig. 10 Isotopic distribution of light olefins formed in the $^{12}C/^{13}C$-methanol switch experiments and the observed isotopomer distribution of hexaMB over AlPO-18 and SAPO-18 catalysts compared with the random one calculated from the same ^{13}C content; the isotopic switch experiments: continuous flow ^{12}C-methanol conversion for 25 min followed by continuous flow ^{13}C-methanol conversion for 1 min over AlPO-18 at 400 °C and SAPO-18-1 and SAPO-18-2 at 300 °C. Experimental conditions: WHSV = 2 h^{-1}; catalyst weight = 100 mg.

mainly follows the olefin methylation and cracking mechanism.[27,38] The large difference in the ^{13}C contents of the olefin products and confined organic materials over AlPO-18 also suggests that olefins are much more involved in the reaction of ^{13}C-methanol than the retained materials (pentaMB and hexaMB). The detailed isotopomer distribution indicates that over AlPO-18 without Brønsted acid sites, ethene molecules containing two ^{13}C atoms, propene molecules containing three ^{13}C atoms, and butene molecules containing four ^{13}C atoms appear as the main olefins. Comparatively, for hexaMB confined in AlPO-18, most of the isotopomers contain less than 6 ^{13}C atoms, indicating that the reactivity of hexaMB is very low. ^{13}C MAS NMR studies over AlPO-18 also show that no carbenium ions are detected over AlPO-18.

All of these findings indicate that the aromatic-based HP mechanism is not the dominating reaction route of the MTO reaction over the AlPO-18 catalyst and that the olefin methylation and cracking mechanism is responsible for the olefin production from methanol over AlPO-18 without Brønsted acid sites. This is different from the mechanism of olefin formation over SAPO-18. For the SAPO-18-2 catalyst with the highest Brønsted acid site density among the three catalysts, the HP mechanism is the dominant route for olefin generation, while for SAPO-18-1 with relatively low Brønsted acid site density, both of the two olefin formation routes, aromatic-based HP mechanism and olefin methylation and cracking mechanism, are feasible.

As a summary, catalyst acidity has a great effect on the mechanism of methanol conversion to light olefins. When the Brønsted acid site density of the catalyst employed is very low (*e.g.* AlPO-18), the formation of HP species is relatively difficult; consequently, the olefin methylation and cracking mechanism becomes the main reaction route for product generation from methanol conversion. Along with the increase of Brønsted acid site density, more polymethylbenzenes are formed and methanol is converted to light olefins mainly through the aromatic-based HP mechanism.

4. Conclusion

In the present study, methanol transformation over AlPO-18 and SAPO-18 was investigated to elucidate the effect of Brønsted acid site density on the reaction mechanism. The methanol conversion was improved over the catalysts with higher Brønsted acid site density. Even with the difference in the catalytic activity of the three catalysts, propene was always predominantly formed among the products, and ethene selectivity was always comparable with butene selectivity and lower than propene selectivity. The pentaMCP$^+$ cation was directly observed over SAPO-18 catalysts under real MTO reaction conditions, but no carbenium ion was observed over AlPO-18 without Brønsted acid sites. Higher Brønsted acid site density favoured the formation and accumulation of important HP species, such as pentaMCP$^+$ and polymethylbenzenes. $^{12}C/^{13}C$-methanol isotopic switch experiments confirmed that polymethylbenzenes were largely formed over SAPO-18 with relatively high Brønsted acid site density and were much more involved in the olefin product generation. The higher reactivity of polymethylbenzenes further proved the feasibility of methanol conversion following the aromatic-based HP mechanism over SAPO-18. The slight difference of ^{13}C incorporation into confined aromatics and olefin products implied that the olefin methylation and cracking mechanism route cannot be ruled out for methanol conversion over SAPO-18 with relatively low Brønsted acid site density. Over AlPO-18 without Brønsted acid sites, olefins are much more reactive towards ^{13}C-methanol than the retained pentaMB and hexaMB and methanol conversion mainly follows the olefin methylation and cracking reaction mechanism. The role of the two mechanisms in the conversion of methanol to light olefins is strongly influenced by the Brønsted acid site density of the catalyst used.

Acknowledgements

The authors thank the financial support from the National Natural Science Foundation of China (no. 21273005, 21273230 and 21103180).

Notes and references

1 M. Stocker, *Microporous Mesoporous Mater.*, 1999, **29**, 3–48.
2 J. F. Haw, W. G. Song, D. M. Marcus and J. B. Nicholas, *Acc. Chem. Res.*, 2003, **36**, 317–326.
3 U. Olsbye, M. Bjorgen, S. Svelle, K. P. Lillerud and S. Kolboe, *Catal. Today*, 2005, **106**, 108–111.
4 W. Wang, Y. J. Jiang and M. Hunger, *Catal. Today*, 2006, **113**, 102–114.
5 J. L. White, *Catal. Sci. Technol.*, 2011, **1**, 1630–1635.
6 D. Chen, K. Moljord and A. Holmen, *Microporous Mesoporous Mater.*, 2012, **164**, 239–250.
7 U. Olsbye, S. Svelle, M. Bjorgen, P. Beato, T. V. W. Janssens, F. Joensen, S. Bordiga and K. P. Lillerud, *Angew. Chem., Int. Ed.*, 2012, **51**, 5810–5831.
8 K. Hemelsoet, J. V. D. Mynsbrugge, K. D. Wispelaere, M. Waroquier and V. V. Speybroeck, *ChemPhysChem*, 2013, **14**, 1526–1545.
9 S. Ilias and A. Bhan, *ACS Catal.*, 2013, **3**, 18–31.
10 G. Seo, J. H. Kim and H. G. Jang, *Catal. Surv. Asia*, 2013, **17**, 103–118.
11 S. Teketel, M. W. Erichsen, F. L. Bleken, S. Svelle and K. Petter, *Specialist Periodical Reports: Catalysis*, 2014, vol. 26, pp. 179–217.
12 G. Ondrey, *Chem. Eng.*, 2011, **118**, 16–20.
13 D. Lesthaeghe, V. Van Speybroeck, G. B. Marin and M. Waroquier, *Angew. Chem., Int. Ed.*, 2006, **45**, 1714–1719.
14 D. M. Marcus, K. A. McLachlan, M. A. Wildman, J. O. Ehresmann, P. W. Kletnieks and J. F. Haw, *Angew. Chem., Int. Ed.*, 2006, **45**, 3133–3136.
15 D. Lesthaeghe, V. Van Speybroeck, G. B. Marin and M. Waroquier, *Ind. Eng. Chem. Res.*, 2007, **46**, 8832–8838.
16 I. M. Dahl and S. Kolboe, *Catal. Lett.*, 1993, **20**, 329–336.
17 I. M. Dahl and S. Kolboe, *J. Catal.*, 1994, **149**, 458–464.
18 I. M. Dahl and S. Kolboe, *J. Catal.*, 1996, **161**, 304–309.
19 W. G. Song, J. F. Haw, J. B. Nicholas and C. S. Heneghan, *J. Am. Chem. Soc.*, 2000, **122**, 10726–10727.
20 B. Arstad and S. Kolboe, *J. Am. Chem. Soc.*, 2001, **123**, 8137–8138.
21 B. Arstad and S. Kolboe, *Catal. Lett.*, 2001, **71**, 209–212.
22 M. Bjorgen, F. Bonino, S. Kolboe, K. P. Lillerud, A. Zecchina and S. Bordiga, *J. Am. Chem. Soc.*, 2003, **125**, 15863–15868.
23 S. Svelle, F. Joensen, J. Nerlov, U. Olsbye, K. P. Lillerud, S. Kolboe and M. Bjorgen, *J. Am. Chem. Soc.*, 2006, **128**, 14770–14771.
24 M. Bjorgen, S. Svelle, F. Joensen, J. Nerlov, S. Kolboe, F. Bonino, L. Palumbo, S. Bordiga and U. Olsbye, *J. Catal.*, 2007, **249**, 195–207.
25 S. Svelle, U. Olsbye, F. Joensen and M. Bjorgen, *J. Phys. Chem. C*, 2007, **111**, 17981–17984.
26 S. Teketel, S. Svelle, K. P. Lillerud and U. Olsbye, *ChemCatChem*, 2009, **1**, 78–81.
27 S. Teketel, U. Olsbye, K. P. Lillerud, P. Beato and S. Svelle, *Microporous Mesoporous Mater.*, 2010, **136**, 33–41.
28 D. M. McCann, D. Lesthaeghe, P. W. Kletnieks, D. R. Guenther, M. J. Hayman, V. Van Speybroeck, M. Waroquier and J. F. Haw, *Angew. Chem., Int. Ed.*, 2008, **47**, 5179–5182.
29 D. Lesthaeghe, A. Horre, M. Waroquier, G. B. Marin and V. Van Speybroeck, *Chem. – Eur. J.*, 2009, **15**, 10803–10808.
30 D. Lesthaeghe, J. Van der Mynsbrugge, M. Vandichel, M. Waroquier and V. Van Speybroeck, *ChemCatChem*, 2011, **3**, 208–212.
31 K. De Wispelaere, K. Hemelsoet, M. Waroquier and V. Van Speybroeck, *J. Catal.*, 2013, **305**, 76–80.
32 C. M. Wang, Y. D. Wang and Z. K. Xie, *Catal. Sci. Technol.*, 2014, DOI: 10.1039/C4CY00262H.
33 J. B. Nicholas and J. F. Haw, *J. Am. Chem. Soc.*, 1998, **120**, 11804–11805.
34 J. Z. Li, Y. X. Wei, J. R. Chen, P. Tian, X. Su, S. T. Xu, Y. Qi, Q. Y. Wang, Y. Zhou, Y. L. He and Z. M. Liu, *J. Am. Chem. Soc.*, 2012, **134**, 836–839.
35 S. T. Xu, A. M. Zheng, Y. X. Wei, J. R. Chen, J. Z. Li, Y. Y. Chu, M. Z. Zhang, Q. Y. Wang, Y. Zhou, J. B. Wang, F. Deng and Z. M. Liu, *Angew. Chem., Int. Ed.*, 2013, **52**, 11564–11568.
36 J. Z. Li, Y. X. Wei, S. T. Xu, P. Tian, J. R. Chen and Z. M. Liu, *Catal. Today*, 2014, **226**, 47–51.
37 M. Bjorgen, F. Joensen, K. P. Lillerud, U. Olsbye and S. Svelle, *Catal. Today*, 2009, **142**, 90–97.
38 J. Z. Li, Y. X. Wei, Y. Qi, P. Tian, B. Li, Y. L. He, F. X. Chang, X. D. Sun and Z. M. Liu, *Catal. Today*, 2011, **164**, 288–292.
39 X. Wang, W. L. Dai, G. J. Wu, L. D. Li, N. J. Guan and M. Hunger, *Catal. Sci. Technol.*, 2014, **4**, 688–696.
40 W. L. Dai, X. Wang, G. J. Wu, N. J. Guan, M. Hunger and L. D. Li, *ACS Catal.*, 2011, **1**, 292–299.
41 W. L. Dai, M. Scheibe, N. J. Guan, L. D. Li and M. Hunger, *ChemCatChem*, 2011, **3**, 1130–1133.
42 W. L. Dai, X. Wang, G. J. Wu, L. D. Li, N. J. Guan and M. Hunger, *ChemCatChem*, 2012, **4**, 1428–1435.
43 M. W. Erichsen, S. Svelle and U. Olsbye, *J. Catal.*, 2013, **298**, 94–101.
44 M. W. Erichsen, S. Svelle and U. Olsbye, *Catal. Today*, 2013, **215**, 216–223.
45 J. S. Chen, J. M. Thomas, P. A. Wright and R. P. Townsend, *Catal. Lett.*, 1994, **28**, 241–248.
46 J. S. Chen, P. A. Wright, J. M. Thomas, S. Natarajan, L. Marchese, S. M. Bradley, G. Sankar, C. R. A. Catlow, P. L. Gaiboyes, R. P. Townsend and C. M. Lok, *J. Phys. Chem.*, 1994, **98**, 10216–10224.
47 D. M. Marcus, W. G. Song, L. L. Ng and J. F. Haw, *Langmuir*, 2002, **18**, 8386–8391.

48 D. S. Wragg, D. Akporiaye and H. Fjellvag, *J. Catal.*, 2011, **279**, 397–402.
49 M. Guisnet, *J. Mol. Catal. A: Chem.*, 2002, **182**, 367–382.
50 M. Guisnet, L. Costa and F. R. Ribeiro, *J. Mol. Catal. A: Chem.*, 2009, **305**, 69–83.
51 Y. X. Wei, J. Z. Li, C. Y. Yuan, S. T. Xu, Y. Zhou, J. R. Chen, Q. Y. Wang, Q. Zhang and Z. M. Liu, *Chem. Commun.*, 2012, **48**, 3082–3084.
52 J. R. Chen, J. Z. Li, Y. X. Wei, C. Y. Yuan, B. Li, S. T. Xu, Y. Zhou, J. B. Wang, M. Z. Zhang and Z. M. Liu, *Catal. Commun.*, 2014, **46**, 36–40.
53 P. W. Goguen, T. Xu, D. H. Barich, T. W. Skloss, W. G. Song, Z. K. Wang, J. B. Nicholas and J. F. Haw, *J. Am. Chem. Soc.*, 1998, **120**, 2650–2651.
54 W. G. Song, J. B. Nicholas and J. F. Haw, *J. Phys. Chem. B*, 2001, **105**, 4317–4323.

